

Nanoscratching-induced phase transformation of monocrystalline silicon –the depth-of-cut effect

Kausala Mylvaganam^{1, a}, L.C. Zhang^{2, b}

¹School of Aerospace, Mechanical and Mechatronic Engineering,
The University of Sydney, NSW 2006, Australia

² School of Mechanical and Manufacturing,
The University of New South Wales, NSW 2052, Australia

^ak.mylvaganam@usyd.edu.au, ^bLiangchi.zhang@unsw.edu.au

Keywords: Silicon, scratching, molecular dynamics, phase transformation.

Abstract. This paper explores the effect of the depth-of-cut of an indenter on the phase transformations during nanoscratching on monocrystalline silicon on the Si(100) orientation. The analysis was carried out by molecular dynamics simulations. It was found that the depth-of-cut and the impingement direction of the indenter had a significant influence on the phase transformations in the initial impression region. At a relatively low depth-of-cut, only amorphous silicon was formed on the scratched surface. When the indenter impinged on a silicon surface with an angle, a bct5-Si crystalline phase in the initial impression region would emerge.

Introduction

The deformation mechanisms of silicon under mechanical loading have been studied extensively. During nano/micro indentation, a series of investigations, both theoretical [1-5] and experimental [6-11] have identified various stable and unstable phases. In our recent nanoindentation study using molecular dynamics (MD) [12], we found that the deformation of silicon during loading depends on the size of the indenter tip. The microstructural evolution during loading and unloading under an indenter of radius 7.5 nm was found to be very different from those with smaller indenters and in excellent quantitative agreement with experimental measurement.

Li et al. [13] reported that dry sliding of single crystal silicon under elastic and elasto-plastic deformation and fracture loading conditions would result in the scratched track with a number of phases including Si-I, Si-III, Si-XII and amorphous Si. Wu et al. [14] investigated the structural variations during nanoscratching with different loads using transmission electron microscopy (TEM) and Raman spectroscopy. They reported that at greater loads, nanocrystals were found within the amorphous silicon region generated by nano scratching and concluded that the phase transformation routes in nanoscratching are different from those in nanoindenting.

Previous MD studies showed that amorphous phase transformation was the main deformation of silicon when subjected to contact sliding [15,16]. However those studies were performed under very shallow depths-of-cut under relatively low loads using a very small indenter. In the present study we will use a larger indenter to make greater depth-of-cut to explore the microstructural changes during scratching.

Molecular dynamics modeling

Molecular dynamics method was used to simulate the scratching on Si(100) surface using a hemi-spherical diamond tip of radius 7.5 nm. Large silicon samples of size 57.02 X 15.20 X 5.97 nm³ and 37.47 X 15.20 X 9.77 nm³ were used in the modeling. Two layers of thermostat atoms and boundary atoms were arranged to surround the Newtonian atoms of silicon to ensure reasonable outward heat conduction during sliding and to eliminate the rigid body motion. Interactions among

silicon atoms were described by Tersoff potential and those among silicon and diamond atoms were described by a modified Morse potential, as explained elsewhere [1-3, 15]. The diamond tip was placed 0.3 nm above the silicon (100) surface and the scratching simulations were done at different depths-of-cut, d , varying from 1 to 2 nm on fresh samples by moving the tip with a speed of 40 m/s, where the depth-of-cut is considered as the penetration of the tip measured from the surface of the workpiece assuming that the surfaces are defined by the envelopes at the theoretical radii of their surface atoms. Two ways of diamond tip impingement were examined. The first (in the case of depths-of-cut = 1, 1.5 and 2 nm, respectively), Impinging 1, was to indent the tip vertically before scratching motion. The second (depth-of-cut = 2 nm), Impinging 2, was to indent and scratch at the same time before reaching the specified depth-of-cut. Hence, the two ways of tip impingement will create different stress fields in the workpiece initial impression regions. These test conditions are summarized in Table 1.

Table 1: Computational test conditions

Impinging Method	Depth of cut, d [nm]	Scratching speed [m/s]
1. Indent up to d , then scratch at the constant depth d	1.0, 1.5, 2.0	40
2. Indent and scratch up to d , then scratch at the constant depth d	2.0	40

Results and Analysis

The cases with the depths-of-cut of 1 nm and 1.5 nm resulted in the maximum normal loads of 0.69 and 0.95 μN respectively. Figs 1(a) and (b) shows the portions of the cross-sectional view of the scratched regions.

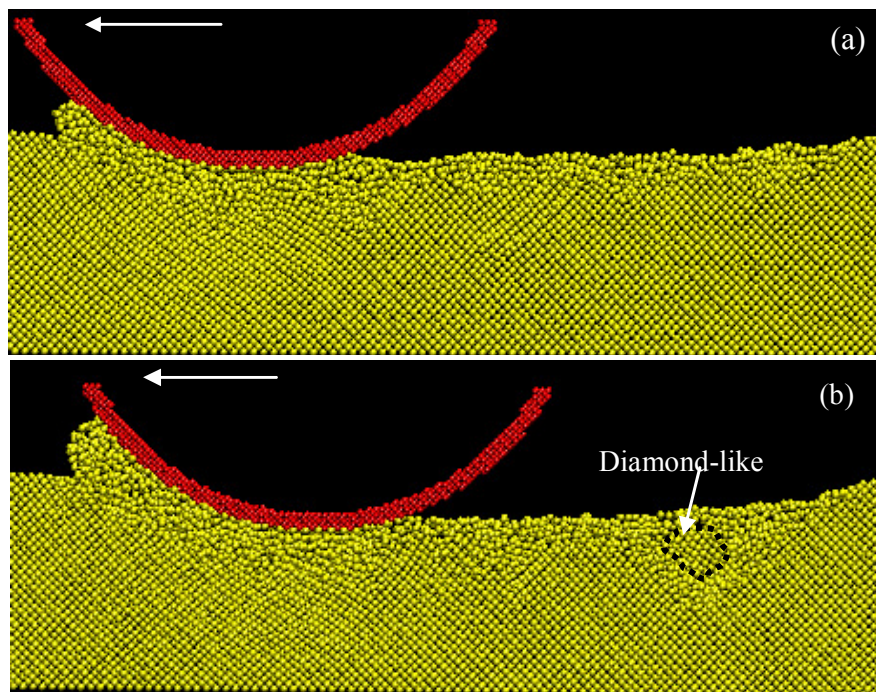


Fig. 1 Portions of the cross-sectional view of the scratched silicon workpiece under a depth-of-cut of (a) 1 nm and (b) 1.5 nm.

The scratching with the 1 nm depth-of-cut led to a thin layer (~ 0.5 nm thickness) of amorphous silicon in the subsurface. Whereas that with the 1.5 nm depth-of-cut resulted in the formation of a diamond-like crystalline phase within the amorphous silicon in the initial impression region and the

scratched surface had several layers of amorphous atoms. Clearly, the thickness of the amorphous layer increased with the depth-of-cut.

In the initial impression region under load, the material deformed up to a depth of 4.5 nm with the emergence of five-coordinated silicon. If the tip was unloaded completely without a scratching motion, the deformed region will return to diamond crystalline structure with a very little residual deformation at the top surface.

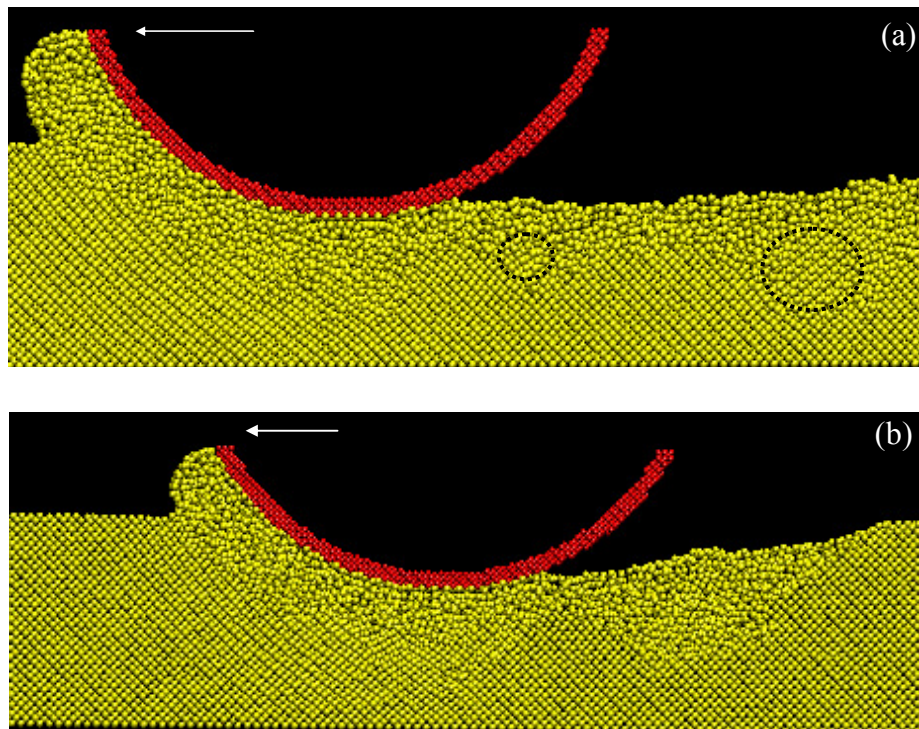


Fig. 2 Portions of the cross-sectional view of the scratched silicon workpiece under 2 nm depth-of-cut made in the way of (a) Impinging 2 (circled region shows a five-coordinated patch), and (b) Impinging 1.

Figs 2(a) and (b) shows the cross-sectional views of the silicon workpiece when scratched with a 2 nm depth-of-cut that introduced a load of $1.2 \mu\text{N}$, in both the ways of Impinging 1 and Impinging 2. Clearly these two initial impression directions resulted in different deformation patterns on scratching. When scratching with the manner of Impinging 2, the deformed atoms in the initial impression region formed an ordered crystalline phase. A detailed analysis showed that these atoms are mainly 5-coordinated with one neighbour at a distance of 2.3 \AA and 4 neighbours at an average distance of $\sim 2.45 \text{ \AA}$, similar to the bct-5 Si identified [4,17] in indentation studies. A portion of this region is shown in Fig. 3.

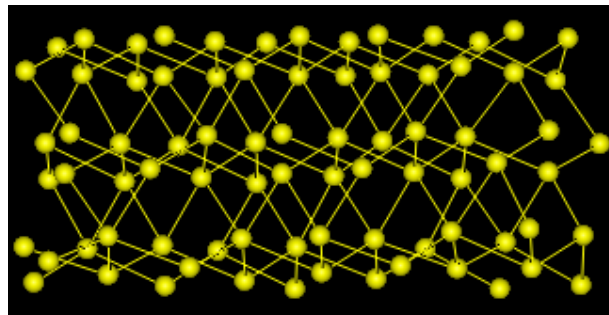


Fig. 3 Portion of the crystalline 5-coordinated atoms in the initial impression region while scratching along the surface.

The scratched surface consists of amorphous atoms for a depth of $\sim 1.2 \text{ nm}$ and some patches of five coordinated atoms under the amorphous atoms. One of these patches is circled in Fig. 2(a). On

the other hand, the scratching made in the manner of Impinging 1 led to a region of mainly amorphous atoms with little crystalline patches in the initial impression region as shown in Fig. 2(b). In both cases the load is nearly the same. The different phase transformation pattern could be due to the differences in stress field variations caused by the ways of tip impingement. The above results are summarized in Table 2.

Table 2 Summary of the results on scratching

Method	Depth of cut [nm]	Normal load [μN]	Phases formed
Impinging 1	1.0	0.69	Amorphous Si
	1.5	0.95	Amorphous & diamond-like Si
	2.0	1.2	Amorphous & diamond-like Si
Impinging 2	2.0	1.2	Amorphous & bct-5 Si

Under the highest load applied in this study, the scratched track consists mainly of amorphous atoms with an averaged bond length of ~ 2.4 to 2.6 Å. However, the formation of randomly oriented Si-I nanocrystals within the amorphous silicon, as reported by Wu et al., cannot be ruled out because unloading from the vertical depth-of-cut of 2 nm, without scratching, clearly resulted in such nanocrystals within the amorphous silicon as shown in Fig. 4.

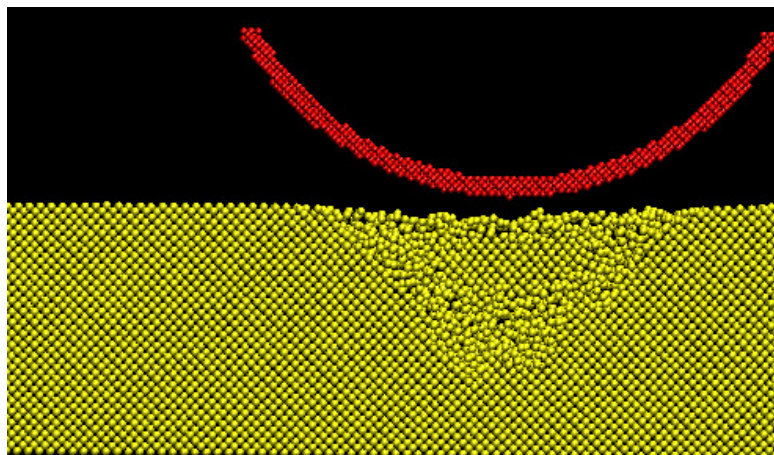


Fig. 4: Portion of the cross-sectional view of silicon when unloaded from 2 nm vertical depth-of-cut, without scratching.

We found that this crystalline phase was made up by the nucleation of the small crystal patches existed at loading and by the transformation of some five-coordinated atoms surrounding these patches during unloading. This mechanism is different from that proposed by Wu et al. on scratching.

Conclusions

Based on the comparison of scratching under different depths-of-cut, we can draw the following conclusions.

- (i) the depth-of-cut and the impingement direction of the indenter has a significant influence on the phase transformation in the initial impression region of a scratch.
- (ii) the inclined impingement resulted in bct5-Si crystalline phase in the initial impression region upon scratching.

Acknowledgement

The authors thank the Australian Research Council for its continuous financial support. This work was also supported by the Australian partnership for advanced computing.

References

- [1] L.C. Zhang, H. Tanaka: JSME Int. J. Series A 42 (1999), p. 546.
- [2] W.C.D. Cheong, L.C. Zhang: Nanotechnology 11 (2000), p. 173.
- [3] W.C.D. Cheong, L.C. Zhang: J. Mater. Sci. Lett. 19 (2000), p. 439.
- [4] D.E. Kim, S.I. Oh: Nanotechnology 17 (2006), p. 2259.
- [5] Y.-H. Lin, S.-R. Jian, Y.-S. Lai, P.-F. Yang: Nanoscale Res. Lett. 3 (2008), p. 71.
- [6] J.Z. Hu, L.D. Merkle, C.S. Menoni, I.L. Spain: Phys. Rev. B 34 (1986), p. 4679.
- [7] M.I. McMahon, R.J. Nelmes, N.G. Wright, D.R. Allan: Phys. Rev. B 50 (1994), p. 739.
- [8] M. Hanfland, U. Schwarz, K. Syassen, K. Takemura: Phys. Rev. Lett. 82 (1999), p. 1197.
- [9] I. Zarudi, L.C. Zhang, J. Zou, T. Vodenitcharova: J. Mater. Res. 19 (2004), p. 332.
- [10] I. Zarudi, L.C. Zhang: Tribol. Int. 32 (1999), p. 701.
- [11] I. Zarudi, J. Zou, L.C. Zhang: Appl. Phys. Lett. 82 (2003), p. 874.
- [12] K. Mylvaganam, L.C. Zhang: Nanotechnology (under review).
- [13] X.C. Li, J.J. Lu, Z.H. Wan, J.H. Meng, S.R. Yang: Tribol. Int. 40 (2007), p. 360.
- [14] Y.Q. Wu, H. Huang, J. Zou, Y. Wang, Q.J. Ren, Z.H. Chen, X.C. Shen, L.C. Zhang: Nanotechnology (under review).
- [15] L.C. Zhang: H. Tanaka, Tribol. Int. 31 (1998), p. 425.
- [16] L.C. Zhang, K. Mylvaganam: J. Computational and Theoretical Nanoscience 3 (2006), p. 167.
- [17] L.L. Boyer, E. Kaxiras, J.L. Feldman, J.Q. Broughton, M.J. Mehl: Phys. Rev. Lett. 67 (1991), p. 715.

Advances in Abrasive Technology XII

10.4028/www.scientific.net/AMR.76-78

Nanoscratching-Induced Phase Transformation of Monocrystalline Silicon – The Depth-of-Cut Effect

10.4028/www.scientific.net/AMR.76-78.387

DOI References

[2] W.C.D. Cheong, L.C. Zhang: Nanotechnology 11 (2000), p. 173.

doi:10.1088/0957-4484/11/3/307

[3] W.C.D. Cheong, L.C. Zhang: J. Mater. Sci. Lett. 19 (2000), p. 439.

doi:10.1023/A:1006707325288

[4] D.E. Kim, S.I. Oh: Nanotechnology 17 (2006), p. 2259.

doi:10.1088/0957-4484/17/9/031

[5] Y.-H. Lin, S.-R. Jian, Y.-S. Lai, P.-F. Yang: Nanoscale Res. Lett. 3 (2008), p. 71.

doi:10.1007/s11671-008-9119-3

[8] M. Hanfland, U. Schwarz, K. Syassen, K. Takemura: Phys. Rev. Lett. 82 (1999), p. 1197.

doi:10.1103/PhysRevLett.82.1197

[10] I. Zarudi, L.C. Zhang: Tribol. Int. 32 (1999), p. 701.

doi:10.1016/S0301-679X(99)00103-6

[13] X.C. Li, J.J. Lu, Z.H. Wan, J.H. Meng, S.R. Yang: Tribol. Int. 40 (2007), p. 360.

doi:10.1016/j.triboint.2005.09.022

[15] L.C. Zhang: H. Tanaka, Tribol. Int. 31 (1998), p. 425.

doi:10.1016/S0301-679X(98)00064-4

[16] L.C. Zhang, K. Mylvaganam: J. Computational and Theoretical Nanoscience 3 (2006), p. 167.

doi:10.1166/jctn.2006.012